

Synthesis and performance evaluation of magnetorheological fluid for continuous flow finishing process

Vinod Chauhan, Mukul Kataria*, Ashwani Kumar, Radhey Sham

Chandigarh College of Engineering and Technology (Degree Wing), Chandigarh 160019, India

Received: 20 February 2024; Accepted: 24 May 2024

In this study, Magnetorheological (MR) finishing fluid samples have been synthesized and experiments have been conducted to investigate the rheological properties namely off-state viscosity and on-state yield stress of prepared samples. The compositions of the MR finishing fluid have been determined by using Taguchi based design of experiment approach. The MR properties have been characterized on a rheometer, using MR device accessory. Bingham Plastic, Casson fluid and Herschel Bulkley are the three fluid models utilized for the modelling of the fluid. The Herschel–Bulkley model has resulted as the most apposite model for fluid with the highest coefficient of regression (R^2) value i.e., 0.9049. Further, Technique for order of preference by similarity to ideal solution (TOPSIS) has also been utilized to establish the effect of its constituents on both the considered rheological properties. To determine the magnetic saturation of the developed MR finishing fluid, graphs between magnetic field strength and on-state yield stress have been plotted. Analysis of Variance (ANOVA) publicized the weight percentage of Fe powder as the most notable parameter, contributing 66.12% followed by the weight percentage of SiC abrasives with 8.09%. The MR finishing fluid samples have attained the highest yield stress at magnetic field intensity of around 0.7 Tesla, which is considered as the limiting value for the finishing process. The optimized fluid sample has been used for finishing 2 mm hole using an indigenously developed finishing process.

Keywords: Finishing, Magnetorheological fluid, Yield shear stress, Viscosity, TOPSIS

1 Introduction

Magnetorheological (MR) fluid is a smart fluid which may alter its rheological property from a freely floating liquid to a semi-solid structure having certain yield shear strength when subjected to magnetic field. The alterations in the rheological behaviour of MR fluid are reversible i.e., after removal of magnetic field, it again converts into the free-flowing liquid^{1,2}. Other characteristics of the MR fluid technology like coalition of input electrical power and output mechanical power, fast response with excellent controllability, has attracted attention of industries, researchers and has resulted in a number of applications³. A system based on the MR fluid technology credibly be the next generation in product design where accuracy, power density and performance will be the decisive features. With time, applications and usages of MR fluid in real-world systems have grown progressively. During the last few years, numerous commercial applications of MR fluid have been developed, e.g., MR fluid surface finishing tools, linear and rotary brakes velocity

control, MR clutches, linear dampers for prosthetic devices, real-time controlled bullet-proof jackets, MR dampers in automobiles for real-time vibration control and in engineering structures for seismic damage mitigation.

MR fluid finishing (MRFF) technique is one of the smart technologies in which the abrading forces are responsible for removing the surface asperities which can be controlled more precisely as compared to conventional finishing processes⁴⁻⁹. A suitable composition of MR finishing fluid may successfully be used to get nano-level finishing without damaging the surface topography of the workpiece¹⁰⁻¹⁴. Continuous flow MRFF is a newly developed finishing process, utilized for finishing the small holes¹⁵. In the continuous flow MRFF process, the off-state viscosity (OSV), as well as on-state yield stress (OSYS) of MR finishing fluid, played significant roles in removing the material from the workpiece surface and achieving the desired process objectives. The OSYS is managed by varying magnetic field intensity in the finishing profile locality, which is produced by the electromagnetic coils whereas the OSV is a function of the fluid composition. The yield stress acquired by the fluid in

*Corresponding author
(Email:mukulkataria89@gmail.com)

the finishing region, where the MR fluid is activated, is accountable for the removal of material from the surface and in rest of the region, the OSV is responsible for the continuous flow of fluid. Having two rheological properties viz. the OSV and the OSYS simultaneously responsible for the feasibility of the continuous flow MRFF process, there must be a need to develop MR fluid having an optimized composition for both these properties, which will result in better machining performance. For this, a multi-criteria decision analysis (MCDA) be employed. The MR finishing fluid generally incorporates ferromagnetic particles and ceramic particles abrasives dispersed into a viscoplastic carrier liquid¹⁶⁻²⁰. The fluid rheological behaviour transforms from a Newtonian fluid to non-Newtonian fluid on exposure to external magnetic field. This change in the rheological property is reversible and in just few milliseconds with the removal of magnetic field²⁰⁻²¹. The non-Newtonian flow behaviour for MR finishing fluid can be determined using different fluid modelling. Generally, Bingham Plastic, Casson's fluid and Hershel–Bulkley models are used for the modelling the fluid²²⁻²³. The ferromagnetic particles of the fluid foster dipole moments and get aligned in the magnetic field direction to turn into columned chains having abrasives embedded in between. The strength of these columned-chained structure is very significant for removing the material from the surface in the MRFF process. So, for optimal performance of any MRFF process, characterization of rheological properties of the used MR finishing fluid has utmost importance²⁴⁻²⁶. The MR fluid's off-state rheological properties are function of fluid composition whereas the on-state rheological properties are function of fluid composition and strength of applied magnetic field. The fluid composition includes the material of its constituents and also the size of its particles, which ultimately control the magnetic properties of the MR fluid²⁷⁻²⁸.

In order to cope up with the rheological necessities of MR fluid for continuous flow MRFF process, it is essential to characterize the MR finishing fluid which is to be indigenously developed. In earlier studies, attempts have been made to explore the on-state properties of MR fluids. But in continuous flow MRFF process, both the off-state as well as on-state rheological properties are to be characterized simultaneously for the better viability of the process. For this, the MR finishing fluid samples are

synthesized and composition of the fluid is optimized for its OSV and OSYS using design of experiment (DOE) based TOPSIS strategy. It is a multi-criterion decision (MCD) technique for selecting an experiment having the optimized results from a finite set of experiments. It is a comprehensive and simple technique having excellent computational efficiency to obtain the relative significance of selected criteria in the methodical form²⁹. Further, the technique is selected after conducting studies on number of available MCDA and defining the problem with mcdai.it. This website provides a tool to select a case specific MCDA method as per the requirement. In this, any multi-criteria decision-making problem can be defined using available options, to obtain a number of analytical MCDA techniques which can be used to solve a particular problem.

2 Materials And Methods

2.1 Synthesis of MR finishing fluid

Carrier liquid, magnetizable particles, abrasives and stabilizer are the four main components of MR finishing fluid. In the present study, silicon oil/deionized water (carrier liquid), pure iron particles (magnetizable particles), green silicon carbide particles (abrasives) and tetra methyl ammonium hydroxide/glycerol (additives) are used to prepare the MR finishing fluid. Pure iron (Fe) powder and green silicon carbide (SiC) powder both of size 600 mesh are used in fluid synthesis as the same size of these particles result in better finishing characteristics. Figure 1 (a) & (b) shows the images of Fe particles and SiC particles respectively which are obtained using Scanning Electron Microscope (SEM). Glycerol is used as an additive for deionized water whereas tetra-methyl-ammonium-hydroxide is utilized for silicon oil.

The MR fluid can be synthesized either with the weight proportion or with the volume proportion of its components. In the present study, the fluid samples

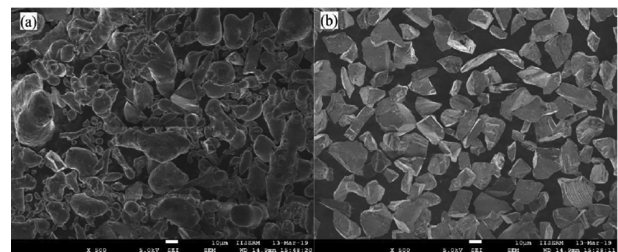


Fig. 1 — SEM images at 500X magnification (a) Fe particles, and (b) SiC particles.

are synthesized using weight proportion. The compositions of various components of fluid are decided based on the literature and its process application i.e., continuous flow MRFF process.

The levels of the compositions are decided with Taguchi design of experiment approach based L_{16} ($3^4 \times 1^2$) orthogonal array (OA). The levels of selected parameters are shown in Table 1. In the weight proportion composition, four levels are selected for iron particles, abrasive particles and carrier medium, while two levels are selected for the type of carrier medium i.e., silicon oil based and deionised water based. The carrier medium is prepared by mixing the carrier liquid and its respective additive in a proportion of 4:1. Taguchi design of experiment using L_{16} OA is represented in Table 2. These sixteen samples are used to determine the optimum combination of MR finishing fluid constituents with OSYS & OSV as response parameters.

The fluid samples are prepared by mixing all the components in a defined order using an electric stirrer. Initially, a homogenous mixture of carrier liquid and the respective additive is prepared and then both the powders are added slowly with simultaneous

stirring to distribute the particles uniformly. Sixteen samples (as per the combinations of L_{16} OA) are then prepared and tested for their rheological properties on a modular compact rheometer (MCR). The error bar graph for repeatability of experimentation is presented in Fig. 2 (a) and (b), I-sign over every bar indicates standard deviation of experiential data for the respective sample. Table 3 shows the mean values for the OSYS and OSV of all sixteen fluid samples.

2.2 Characterization of MR Finishing Fluid Samples

Rheological characteristics of newly developed MR fluid are required before it's used or any application in any process. The determination of OSV and OSYS is necessary to investigate its suitability & effectiveness for a continuous flow MRFF process. The OSYS indicates the bonding strength of abrasive particles into the Fe particle's chains and the shear force which the fluid can exert on the finishing surface at the time of finishing operation; whereas the OSV shows its behaviour in the passage of flow, where there is no magnetic field. In the present study, the fluid is characterized for an indigenously developed continuous flow type of MR fluid finishing

Table 1 — Input parameters along with their values at corresponding levels

Symbol	Input Parameter	Levels				Units
		I	II	III	IV	
A	Weight of Fe Powder	20	25	30	35	gm
B	Weight of SiC Powder	4	6	8	10	gm
C	Weight of carrier medium	50	55	60	65	gm
D	Type of carrier medium	SO based	DIW based	-----	-----	-----

SO: Silicon oil; DIW: Deionized water

Table 2 — L_{16} OA utilized to synthesize the MR finishing fluid samples

Exp. No.	Levels of input parameters				Corresponding values of input parameters			
	A	B	C	D	Fe powder	SiC powder	Carrier medium	Type of carrier medium
1	1	1	1	1	20	4	50	SO
2	1	2	2	1	20	6	55	SO
3	1	3	3	2	20	8	60	DIW
4	1	4	4	2	20	10	65	DIW
5	2	1	2	2	25	4	55	DIW
6	2	2	1	2	25	6	50	DIW
7	2	3	4	1	25	8	65	SO
8	2	4	3	1	25	10	60	SO
9	3	1	3	1	30	4	60	SO
10	3	2	4	1	30	6	65	SO
11	3	3	1	2	30	8	50	DIW
12	3	4	2	2	30	10	55	DIW
13	4	1	4	2	35	4	65	DIW
14	4	2	3	2	35	6	60	DIW
15	4	3	2	1	35	8	55	SO
16	4	4	1	1	35	10	50	SO

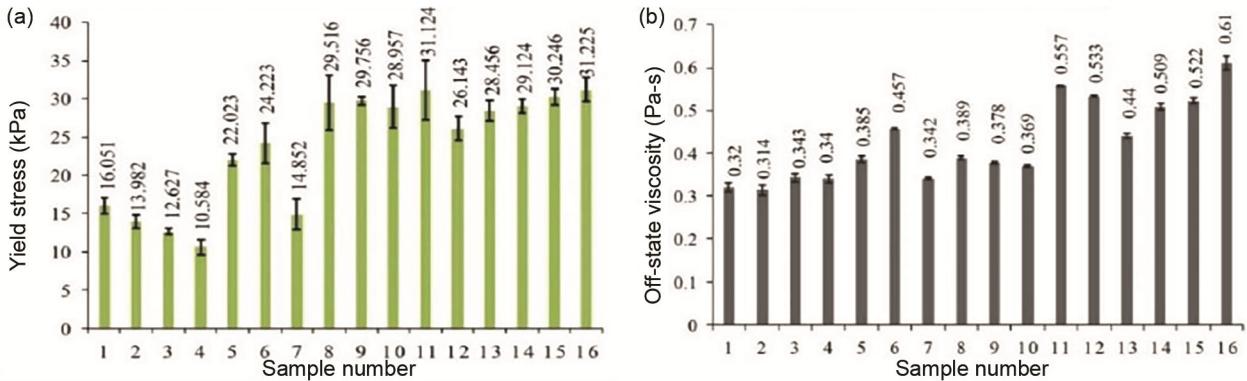


Fig. 2 — Error bar graphs and experimental results for (a) on-state yield stress, and (b) off state viscosity.

Table 3 — Output responses for the MR finishing fluid samples

Exp. No.	Input parameters				Response parameter	
	Fe powder	SiC powder	Carrier medium	Type of carrier medium	Yield stress (kPa)	OSV (Pa-s)
1	20	4	50	SO	16.051	0.320
2	20	6	55	SO	13.982	0.314
3	20	8	60	DIW	12.627	0.343
4	20	10	65	DIW	10.584	0.340
5	25	4	55	DIW	22.023	0.385
6	25	6	50	DIW	24.223	0.457
7	25	8	65	SO	14.852	0.342
8	25	10	60	SO	29.516	0.389
9	30	4	60	SO	29.756	0.378
10	30	6	65	SO	28.957	0.369
11	30	8	50	DIW	31.124	0.557
12	30	10	55	DIW	26.143	0.533
13	35	4	65	DIW	28.456	0.440
14	35	6	60	DIW	29.124	0.509
15	35	8	55	SO	30.246	0.522
16	35	10	50	SO	31.225	0.610

process for obtaining the finishing of small holes. In this developed process, the fluid changes its rheological behaviour (from liquid to solid state) only in a specific region of flow passage where the workpiece having small holes is placed and in rest of the passage, it remains in liquid state. The peristaltic pump receives the fluid in liquid state from the fluid reservoir, so the OSV of the fluid will play an imperative role and the yield stress acquired by the fluid in finishing region will result in the material removal.

Figure 3(a) shows a section of the developed finishing process for MR fluid, while Fig. 3(b) shows the phenomena of material removal in finishing region of the developed process. The MR finishing fluid in the developed process has unidirectional continuous fluid flow which is normal to magnetic flux lines. In the finishing region, the SiC abrasive

particles get entrenched in between the iron particles of the stiffened fluid which apply two forces on the surface asperities, a tangential force (F_t) as a result of the flow of fluid and a normal force (F_n) because of the stiffened fluid in finishing region. The penetration of the abrasives in the surface resulted due to the normal force (F_n) and the shear force (F_t) exerted by the flow of fluid and tear-off the material. So, a higher OSYS results in better penetration of abrasives whereas a large flow imposes a better shear force upon the surface asperities.

The MR finishing fluid samples are characterized using a rheometer (Anton Paar MCR-302). It facilitates variable magnetic field strength upto 1.3 Tesla during testing which is sufficient enough for studying the magnetic saturation of the MR fluid. The magnetic field's direction generated by the MR device accessory in the rheometer is normal to fluid

deformation’s direction that is alike to the continuous flow MRFF process. Figure 4 (a) & 4(b) shows the rheometer and the illustration of the testing process of fluid sample respectively⁶.

2.3 Modelling of fluid samples

The modelling of MR fluid based on its OSV and OSYS is utmost important before using it in an intended application. Three models *viz.* Casson fluid, Herschel Bulkley, Bingham plastic are generally utilized for the modelling of MR fluids³⁰. The results from the fluid testing are used in the constitutive equations of the three models and coefficient of regression (R^2) value is determined to find the best-suited fluid model. The three models assume that the fluid flow starts only after a critical value of shear force, termed as yield stress of the fluid. But after the commencement of the flow, behaviour for each model is unlike.

In Bingham Plastic model, the fluid acts as a resistant body before the commencement of flow, and

after that it follows Newtonian fluid behaviour³¹. The constitutive equation meant for the Bingham Plastic model is given as:

$$\tau = \tau_y + \dot{\gamma} \eta \quad \dots (1)$$

In Herschel-Bulkley fluid model, the fluid having pseudo-plastic properties are characterized using the following relationship³¹:

$$\tau = \tau_y + K\dot{\gamma}^n \quad \dots (2)$$

Casson’s fluid model characterizes the fluid with following relationship³¹:

$$\tau^{1/2} = \tau_y^{1/2} + (\dot{\gamma} \eta_c)^{1/2} \quad \dots (3)$$

where τ is shear stress, τ_y is yield stress, $\dot{\gamma}$ is shear rate, η is viscosity of the fluid, K is consistency index, n denotes power-law index and η_c is Casson’s viscosity.

In Herschel Bulkley's model, value of power index above 1 denotes shear thickening while the value

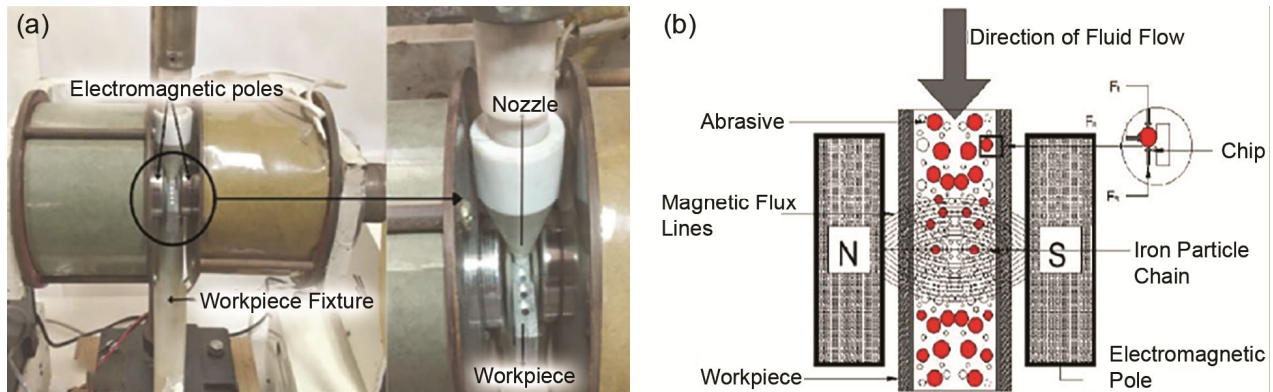


Fig. 3 — (a) Finishing region of the continuous flow MRFF process, and (b) Illustration of MR finishing phenomenon.

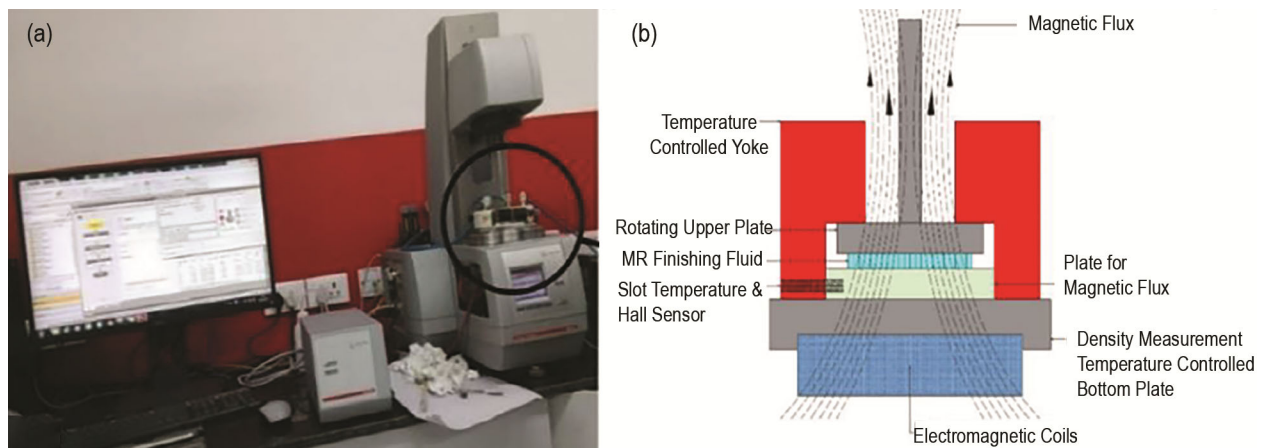


Fig. 4 — (a) Rheometer used for characterization (Anton Paar MCR 302), and (b) illustration of the testing process of characterization of fluid sample.

Table 4 — Modelling of MR finishing fluid samples

Fluid Sample No.	Bingham Model		Herschel-Bulkley			Casson Fluid	
	$\tau = \tau_y + \dot{\gamma}\eta$		$\tau = \tau_y + K\dot{\gamma}^n$			$\tau^{1/2} = \tau_y^{1/2} + (\dot{\gamma}\eta_c)^{1/2}$	
	τ_y (Pa)	η (Pa-s)	τ_y (Pa)	K	N	τ_y (Pa)	η_c (Pa-s)
01	13867.91	222.87	6381.44	3086.41	0.675	9572.21	42.339
02	12679.67	194.33	5841.37	2438.28	0.386	8761.99	36.68
03	12165.98	182.00	5607.87	2158.1	0.752	8411.86	34.16
04	11028.01	154.68	5090.61	1537.38	0.794	7635.91	28.69
05	14495.84	237.94	6666.92	3428.93	0.378	10000.35	45.35
06	16844.91	294.33	7734.61	3940.23	0.883	11602.00	56.63
07	13056.24	203.37	6012.55	2643.69	0.705	9018.81	38.43
08	22571.32	431.81	10337.57	3103.68	0.507	15506.36	84.12
09	24099.58	468.51	11032.24	3937.32	0.705	16548.37	91.46
10	19249.73	352.07	8827.74	3822.02	0.520	13241.65	68.16
11	28258.42	568.35	12922.62	6535.79	0.789	19383.94	111.58
12	17912.50	319.96	8219.92	4192.55	0.711	12329.89	61.75
13	18986.48	345.75	8708.10	3678.36	0.962	13062.16	66.91
14	22362.00	427.44	10242.5	4419.55	0.539	15363.68	83.12
15	26886.45	535.42	12299.01	3147.44	0.921	18448.52	104.85
16	29030.78	586.90	13274.17	4757.08	0.478	18261.36	115.14

below 1 denotes shear thinning behaviour. The consistency index ‘ K ’ represents fluid’s viscosity. In line with Casson’s fluid model, in particulate suspensions, the particles flocculate into rod-like structures and break after attaining critical shear stress. If the shear rate is further increased, the size of these rods reduces till they broke into the primary particles at higher values of shear rates³². The resulting rheological characteristics after analysing the results with the governing equations of the three examined fluid models are represented in Table 4. Figure 5 shows the flow curves of three fluid models. By considering these three fluid models, a typical shear thinning behaviour is noticed for prepared fluid samples.

Coefficient of regression (R^2) is one of the most suitable methods to determine the goodness of fit of a stated model²³. The R^2 value is obtained by substituting the experimental results in the equations of the three models. The average value of the R^2 calculated for Bingham Plastic model is 0.7685, for Casson fluid model is 0.4859 and for Herschel-Bulkley is 0.9049. From the R^2 analysis, it is clear that the MR finishing fluid’s flow behaviour, to be utilized for continuous flow MRFF process, is the most suitably described by the Herschel-Bulkley model. Figure 6 shows a comparison of R^2 values for the three models. The R^2 value in case of Herschel Bulkley fluid model is higher as compared to Casson Fluid and Bingham Plastic models.

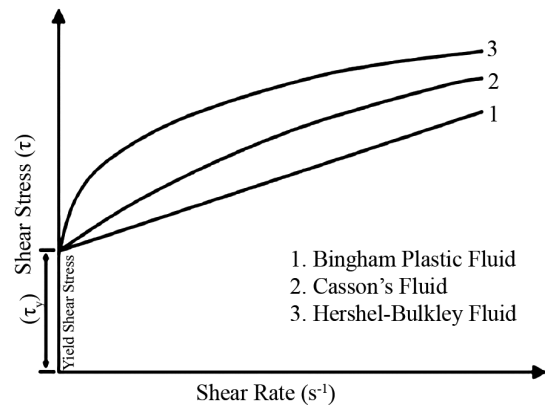


Fig. 5 — Flow behaviour of Bingham Plastic, Casson’s and Herschel-Bulkley fluids.

2.4 Technique for Order of Preference by Similarity to Ideal Solution (TOPSIS)

In a continuous flow MRFF process, control on two properties *viz.* OSYS attained by the fluid and its OSV is necessary for its better feasibility. The on-stress yield stress regulates the finishing operation of holes in the finishing region where magnetic field is present while the OSV REGULATES the continual flow of MR finishing fluid in rest of the region where magnetic field doesn’t exist. For a better performance of the process, the OSYS should have a high value so that more material can be removed from the surface and the OSV should have a low for a continual flow of MR finishing fluid. For lower OSV the Fe particle concentration should be lesser and for higher OSYS the Fe particle concentration should be more. So,

these two fluid properties are required to be optimized using some multi-response optimization technique, for better performance of the process³³⁻³⁴. In the present study, composition of the fluid of the MR finishing fluid is optimized using TOPSIS, considering OSYS and OSV as response parameters.

TOPSIS is a MCDA, used to identify the best solution from a finite set of experiments. It selects the alternatives as per relative closeness to positive idealized solution and distance taken from the negative idealized one in terms of preference values, and ranked each alternative accordingly²⁹. The solution having the maximum preference value, which is also the highest ranked one, is considered to be the best for optimal performance of the process.

A matrix consists of ‘*n*’ aspects (multiple responses for which the study is to be conducted) and ‘*m*’ alternatives (number of experiments of the conducted study) known as decision matrix, is illustrated as Eq. (4)

$$D_m = \begin{bmatrix} x_{11} & x_{12} & x_{13} & \dots & x_{1n} \\ x_{21} & x_{22} & x_{23} & \dots & x_{2n} \\ \vdots & \vdots & \vdots & \ddots & \vdots \\ \vdots & \vdots & \vdots & \ddots & \vdots \\ x_{m1} & x_{m2} & x_{m3} & \dots & x_{mn} \end{bmatrix} \dots (4)$$

where, x_{ij} denotes performance of i^{th} alternative (fluid sample number) with respect to j^{th} aspect (response *i.e.*, on-state yield strength and OSV). The decision matrix in the present study has sixteen rows for each individual fluid sample, and two columns for the two responses *viz.* on-state yield strength and OSV. Normalized matrix is obtained from Eq. (5)

$$r_{ij} = \frac{x_{ij}}{\sqrt{\sum_{i=1}^m x_{ij}^2}} \quad j=1, 2, 3, \dots, n \quad \dots (5)$$

For on-state yield strength $j = 1$ and for OSV $j = 2$; and $i = 1, 2, \dots, 16$ for fluid sample 1 to 16. For fluid sample 1 with OSYS as response, r_{ij} is r_{11} , and so on. The results are shown in Table 5.

Weighted normalized decision matrix $V = [v_{ij}]$ may be obtained by assigning the weight to the individual attribute by using Eq. (6) as:

$$V = w_j r_{ij} \quad \dots (6)$$

where, $\sum_{j=1}^n w_j = 1$. w_1 (= 0.6) is weight given to the OSYS and w_2 is weight given to the OSV having

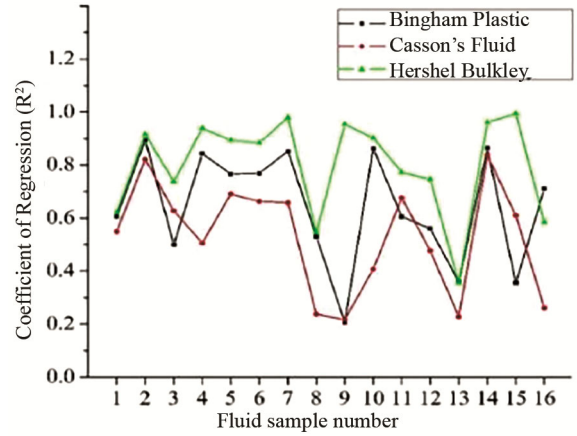


Fig. 6 — Comparison of the R^2 value for the fluid models.

Table 5 — Normalized matrix of performance characteristics

Exp. No.	Response parameter (Decision matrix, D_m)	Normalized		
		$r_{ij} = \left(x_{ij} / \sqrt{\sum_{i=1}^m x_{ij}^2} \right)$		
	Yield Stress (kPa)	OSV (Pa-s)	Yield Stress (r_{i1})	OSV (r_{i2})
1	16.051	0.320	0.1620	0.1838
2	13.982	0.314	0.1411	0.1803
3	12.627	0.343	0.1274	0.1970
4	10.584	0.340	0.1068	0.1953
5	22.023	0.385	0.2223	0.2211
6	24.223	0.457	0.2445	0.2625
7	14.852	0.342	0.1499	0.1964
8	29.516	0.389	0.2979	0.2234
9	29.756	0.378	0.3003	0.2171
10	28.957	0.369	0.2923	0.2119
11	31.124	0.557	0.3142	0.3199
12	26.143	0.533	0.2639	0.3061
13	28.456	0.440	0.2872	0.2527
14	29.124	0.509	0.2940	0.2924
15	30.246	0.522	0.3053	0.2998
16	31.225	0.610	0.3152	0.3504

a value of 0.4. The on-state viscosity has been assigned a higher weight because it is the factor which is mainly responsible for material removal in the continuous flow MRFF process. The positive along with negative-ideal solutions are determined using Eqs. (7) & (8) as:

$$v^+ = (v_1^+, v_2^+, \dots, v_n^+) = \left(\left[\max_i v_{ij} | j \in J \right], \left[\min_i v_{ij} | j \in J \right] \right) \quad i = 1, 2, 3 \dots m \dots (7)$$

$$v^- = (v_1^-, v_2^-, \dots, v_n^-) = \left(\left[\min_i v_{ij} | j \in J \right], \left[\max_i v_{ij} | j \in J \right] \right) \quad i = 1, 2, 3 \dots m \dots (8)$$

The separation between every alternative taken from the ‘ideal solution’ are determined using Eq. (9) as:

$$s_i^+ = \sqrt{\sum_{j=1}^n (v_{ij} - v_j^+)^2} \quad i = 1, 2, 3, \dots, m \quad \dots (9)$$

The separation of every alternative taken from ‘negative-ideal’ solution is determined using Eq. (10) as:

$$s_i^- = \sqrt{\sum_{j=1}^n (v_{ij} - v_j^-)^2} \quad i = 1, 2, 3, \dots, m \quad \dots (10)$$

The respective closeness of the alternative with the ideal solution is calculated by Eq. (11) given as:

$$P_i = \frac{s_i^-}{s_i^+ + s_i^-} \quad i = 1, 2, 3, \dots, m \quad \dots (11)$$

The calculated P_i value is then ranked in a descending sequence to recognize the set of alternatives indicating the most and the least preferred solution.

The optimization of MR finishing fluid composition with multiple performance characteristics *i.e.*, OSV and OSYS is accomplished using TOPSIS. The preference values for all sixteen fluid samples are calculated from both the responses. The normalized matrix (Table 5), weighted normalized decision matrix (Table 6), separation of alternatives from positive & negative ideal solutions and ranking as per the preference values for TOPSIS (Table 7) for each fluid sample are presented. From Table 6, it can be observed that the weight assigned to the OSV (w_2) is 0.4, whereas the weight assigned to OSYS (w_1) is 0.6. The reason for giving higher weight to the yield stress is due to usage of a peristaltic pump in the developed continuous flow MRFF process for fluid circulation through the workpiece hole. In the off-state position, the MR fluid’s viscosity nearly same as that of the carrier medium, which can easily be circulated through the passage using a peristaltic pump, so the OSV has given less weight. But in the on-state condition, the fluid gets stiffened to a solid-like state and at this stage, it is the yield stress acquired by the fluid which is accountable for material removal from workpiece surface. So, it has been given higher weight than OSV.

From the TOPSIS analysis, it is clear that fluid sample 9 has the highest preference value providing the best multiple response characteristics; hence it has the optimal composition of MR finishing fluid, followed by sample 10 and 8. As the highest preference value is considered as the optimum

Table 6 — Weighted Normalized decision matrix of performance characteristic

Exp. No.	Weighted normalized values $\left(\sum_{j=1}^n w_j = 1\right)$	
	Yield stress ($w_1 = 0.6$)	OSV ($w_2 = 0.4$)
1	0.0972	0.0735
2	0.0846	0.0721
3	0.0764	0.0788
4	0.0641	0.0781
5	0.1333	0.0884
6	0.1467	0.1050
7	0.0899	0.0785
8	0.1787	0.0893
9	0.1802	0.0868
10	0.1753	0.0847
11	0.1885	0.1279
12	0.1583	0.1224
13	0.1723	0.1011
14	0.1764	0.1169
15	0.1832	0.1199
16	0.1891	0.1401

Table 7 — Values of alternatives from ideal solutions and ranking as per the preference values

Exp. No.	Response parameter		Preference value $\left(P_i = s_i^- / (s_i^+ + s_i^-)\right)$	Order
	S^+	S^-		
1	0.0919	0.0744	0.4473	12
2	0.1044	0.0710	0.4048	13
3	0.1128	0.0625	0.3567	15
4	0.1251	0.0620	0.3313	16
5	0.0580	0.0864	0.5981	11
6	0.0536	0.0897	0.6259	9
7	0.0993	0.0667	0.4019	14
8	0.0201	0.1254	0.8618	3
9	0.0171	0.1277	0.8814	1
10	0.0186	0.1243	0.8694	2
11	0.0558	0.1250	0.6912	7
12	0.0589	0.0958	0.6191	10
13	0.0334	0.1150	0.7747	4
14	0.0465	0.1146	0.7111	6
15	0.0481	0.1208	0.7149	5
16	0.0680	0.1250	0.6476	8

solution, “third level of parameter A (Fe powder concentration), first level of B (SiC powder concentration), third level of C (carrier medium concentration) and first level of D (type of carrier medium)” offer maximum preference value and are considered to be the optimum set of fluid composition for both the responses *i.e.*, OSV and OSYS. The optimal parametric combination is found to be $A_3B_1C_3D_1$.

Figure 7 (a) shows the plot of preference values for all the sixteen fluid samples. The mean of the performance values for all the levels of the fluid component is calculated and summarized in Table 8. Larger mean performance value presents closer response quality to the ideal value. It is clear from the Table that weight percentage of *Fe* powder has ranked first in deciding the selected multiple responses followed by weight percentage of *SiC* abrasives, weight percentage of carrier medium and type of carrier medium respectively. Therefore, larger performance value is preferred for the optimal performance. Based on the study, the levels of input parameters at higher on-state yield strength handlower OSV are $A_3B_1C_3D_1$. Figure 7 (b) shows the plot of preference values in accordance with all the levels of input parameters.

2.5 Taguchi Design of Experiment Based Analysis

The data for mean preference value (Table 7) and preference value for all the levels of input parameters i.e., *Fe* powder concentration, *SiC* powder concentration, carrier medium concentration at four levels and type of carrier medium at two levels (Table 8), is analyzed using Taguchi based design of

experiment. Response of the analysis for the mean of S/N ratios along with mean of means are shown in Tables 9 & 10 respectively. From these Tables, the highest response for preference value is observed at level 3 for *Fe* powder concentration; level 1 for *SiC* powder concentration, level 3 for carrier medium concentration and level 1 for type of carrier medium concentration. Figure 8 is the graphical representation for mean of means and S/N ratios obtained from the Taguchi design of experimental-based analysis.

Table 11 represents the ANOVA of preference values with the percentage contribution for each input parameter. Fisher’s *F* test is also conducted to identify the remarkableness of input parameters for the performance characteristic. A higher *F*-value states that the variation of input parameter has a remarkable influence on the response characteristic. From *F*-test, it is clear that the *Fe* powder concentration is the most predominant parameter which affects the preference value.

3 Results and Discussion

The prepared MR finishing fluids have been characterized, considering the OSV and OSYS which governs the continuous flow MRFF process. The fluid changes its behaviour only in the finishing region

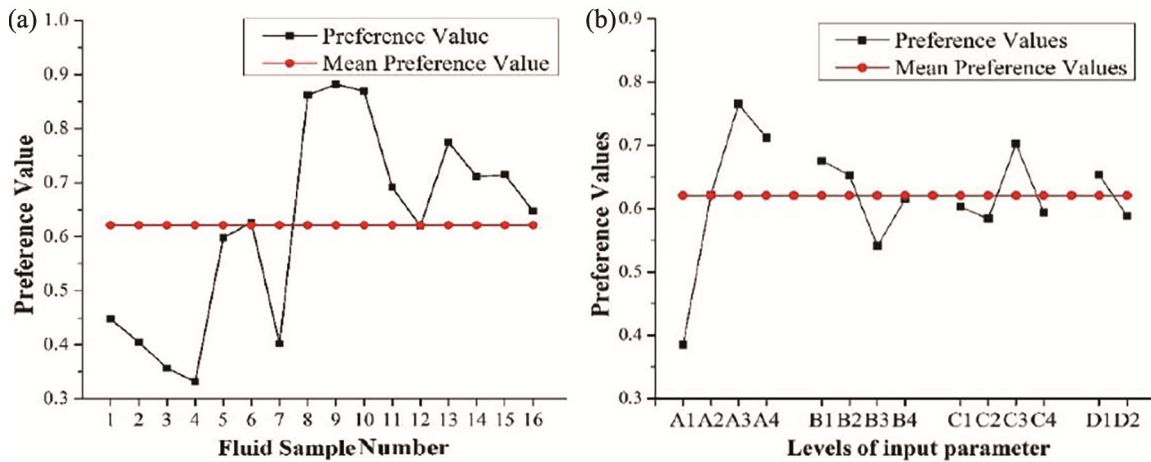


Fig. 7 — (a) Preference values for all the sixteen fluid samples, and (b) Preference values in accordance with each level of the input parameters.

Table 8 — Values of mean of the preference according to the levels of input parameters

Parameter	Levels				Main effect (max. - min.)	Rank
	I	II	III	IV		
Weight of <i>Fe</i> Powder	0.3851	0.6219	0.7653*	0.7121	0.3802	1
Weight of <i>SiC</i> Powder	0.6754*	0.6528	0.5412	0.6150	0.1342	2
Weight of carrier medium	0.6030	0.5842	0.7027*	0.5943	0.1185	3
Type of carrier medium	0.6536*	0.5885	-----	-----	0.0651	4
Mean of preference values = 0.6211						
* Levels for optimum grey rational grade						

Table 9 — Responses for mean of means of preference value

Level	Parameter	Weight of <i>Fe</i> powder	Weight of <i>SiC</i> powder	Weight of carrier medium	Type of carrier medium
I		0.3851	0.6754	0.6031	0.6537
II		0.6220	0.6529	0.5843	0.5886
III		0.7653	0.5421	0.7028	-----
IV		0.7121	0.6150	0.5944	-----
Delta		0.3802	0.1342	0.1185	0.0651
Rank		1	2	3	4

Mean of means of Preference values = 0.6211

Table 10 — Responses for mean of S/N Ratios of preference value

Level	Parameter	Weight of <i>Fe</i> powder	Weight of <i>SiC</i> powder	Weight of carrier medium	Type of carrier medium
I		-8.346	-3.691	-4.509	-4.131
II		-4.435	-4.025	-4.849	-4.954
III		-2.421	-5.748	-3.575	-----
IV		-2.966	-4.705	-5.236	-----
Delta		5.925	2.057	1.66	0.823
Rank		1	2	3	4

Mean of S/N ratios of Preference values = -4.542

Table 11 — ANOVA results for the obtained preference values

Source	DF	Seq. SS	Adj. MS	F-Value	Contribution
Weight of <i>Fe</i> Powder	3	0.33910	0.11303	7.15	66.12%
Weight of <i>SiC</i> Powder	3	0.04151	0.01384	0.88	08.09%
Weight of carrier medium	3	0.03628	0.01209	0.77	07.07%
Type of carrier medium	1	0.01697	0.01697	1.07	03.31%
Error	5	0.07902	0.01580		
Total	15	0.51288			

Model summary: SD = 0.125712; R-square = 94.59%

DF: degree of freedom; MS: mean square and SS: sum of square;

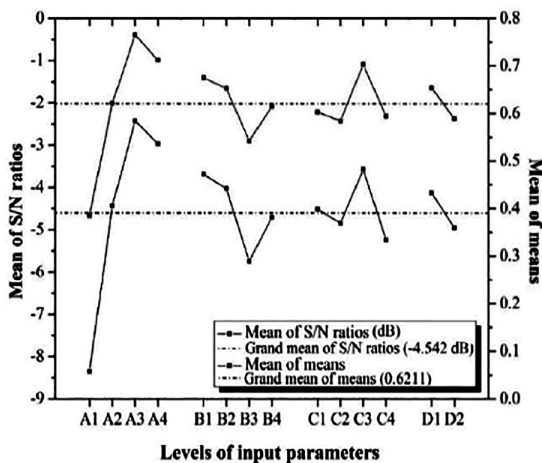


Fig. 8 — Mean of S/N ratios and mean of means for preference values.

where OSYS plays a significant role in removing material from surface and in rest of the regions the off-state properties play important role for its continuous flow. In continuous flow finishing process

through MR finishing fluid, the OSYS of prepared fluid is to be optimum while the OSV is to have lowest value. In MR finishing fluid, the weight percentage of abrasives particle plays an important part in governing the rheological behaviour as abrasive particles serve as a defect site inside iron particles lattice and alter the yield shear stress necessary for initiating the finishing process. OSV and shear rate plots are obtained to realize the fluid's flow behaviour and is featured in Fig. 9 (a). The lowest OSV value obtained is 0.314 Pa-s for sample no. 2 while its highest value is 0.61 Pa-s for sample no. 16.

From these results, it is clear that the ratio of solid content (*Fe* and *SiC* particles) and the carrier medium decides the off-state MR fluid viscosity. The higher ratio signals the greater value of the OSV. Figure 9 (b) shows the variation resulting in the OSYS on alteration of shear rate and the highest value in case of the OSYS is observed to be 31.225 kPa for sample no. 16 whereas its lowest value is 10.584 kPa for sample

no. 4. The results revealed that although the percentage of ferromagnetic iron particles decides the OSYS of MR fluid but it is also affected by non-magnetic *SiC* particles. The non-magnetic *SiC* particles get embedded between chain structured iron particles and hence cessation the strength which can otherwise be attained without their interference. Further, large amount of *SiC* abrasives caused higher discontinuities in the chain structured iron particles and hence resulted in lesser OSYS.

3.1 Effect of Input parameters

Figures 10(a to f) exhibits the interaction curves for variation in both the response parameters, *i.e.* OSV and OSYS. Figures 10(a), (b) & (c) show variation of OSYS and Figs. 10(d), (e) and (f) show the variation of OSV. It is clear from Fig. 10(a) & (b) that weight percentage of iron has a positive impact on the finishing fluid's yield stress, whereas the percentage of carrier medium has an adverse effect.

From Fig. 10(b) & (c), as the weight percentage of carrier medium increases the corresponding yield stress decreases. Figure 10(a) exhibits the reduction in fluid yield strength on increasing the concentration of mixed *SiC* abrasive particles but when the combined effect of carrier medium and *SiC* abrasives is observed from Fig. 10(c) the yield stress gets enhanced on increasing the *SiC* concentration.

From these interaction curves of yield stress, it is clear that the weight percentage of *Fe* powder effects the OSYS positively, whereas both the other parameters share an inverse relation. A higher concentration of carrier medium enhances fluidity of prepared finishing fluid, and the abrasive particles the

disturb continuity of iron particles chains and create defect sites into iron particles lattice that reduces the yield strength.

From Fig. 10(d), (e) and (f), it is clear that the OSV of MR finishing fluid enhances on increasing the weight percentage of *Fe* powder and abrasion particles, whereas it mitigates on increasing weight percentage of the carrier medium.

3.2 Effect of magnetic field strength

Figure 11 shows the dependency of OSYS on intensity of the magnetic field. The plots are drawn to observe the pattern of the OSYS in accordance with the varying magnetic field on a constant 1 s^{-1} of shear rate. The plots show that the finishing fluid's yield increases on increasing the magnetic field strength, but beyond the value of 0.6 T, it becomes almost constant thereafter. This is because the iron particles present in the fluid samples become magnetically saturated. These results play a very significant part in designing the continuous flow finishing process because according to the plot, the variation of the magnetic field can be up to 0.6 T and beyond this there is no significant change in the fluid properties. The highest value of yield stress obtained for fluid sample 9 is 69.72 kPa and for fluid sample 8 is 68.21 kPa at magnetic field of 0.7 T and 0.8 T respectively.

3.3 Performance of the developed MR fluid samples

From the results of this study, it is clear that the OSV of prepared samples ranges from 0.314 Pa-s to 0.610 Pa-s and the on-state yield strength ranges from 10.584 kPa to 31.225 kPa. This signifies that the fluid can be used successfully in a continuous flow

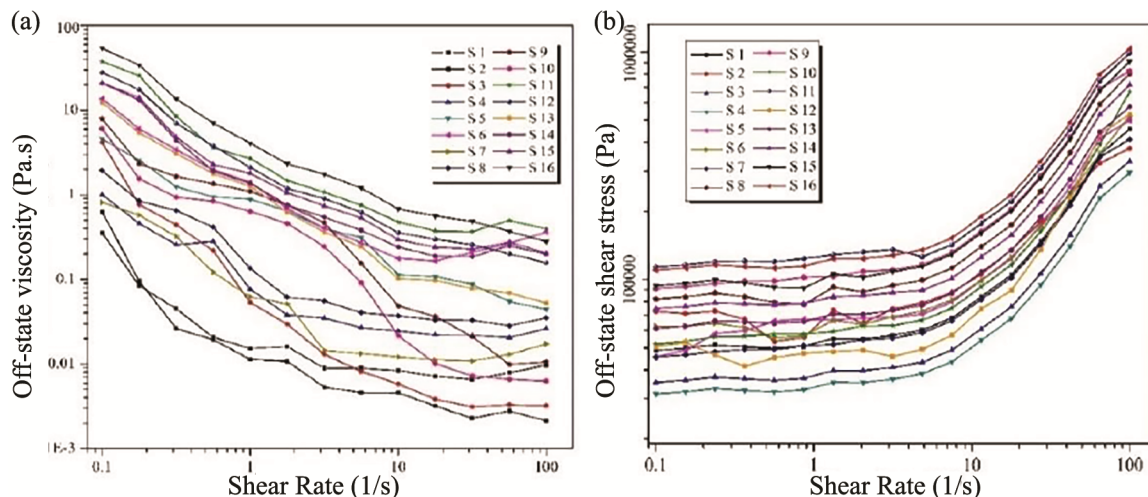


Fig. 9 — (a) Shear rate v/s OSV Plot, and (b) Shear rate v/s OSYS Plot.

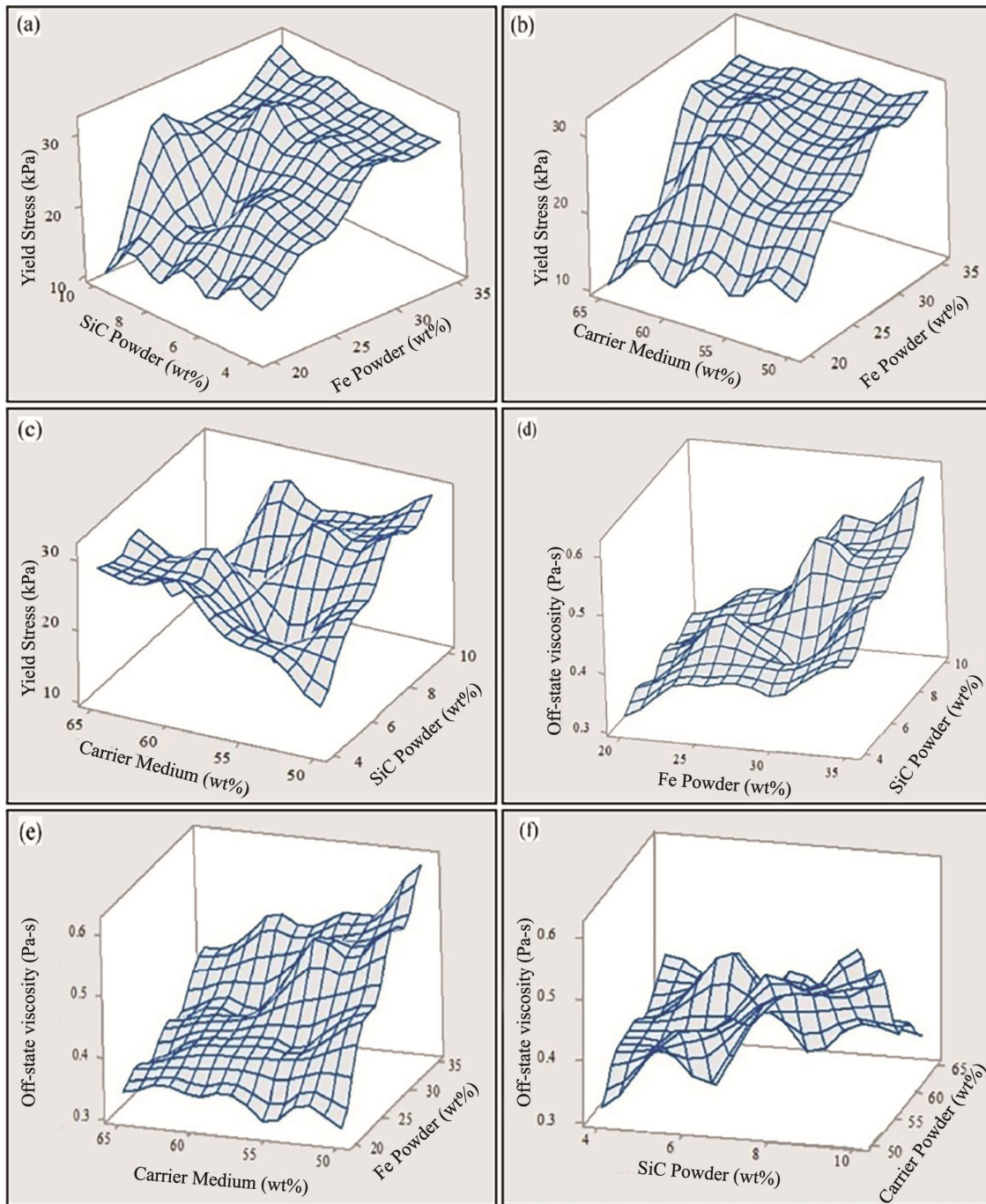


Fig. 10 — Interaction curves for on-state yield stress and off-state viscosity (a) concentration of Fe particles and SiC Particles v/s OSYS, (b) concentration of Fe particles and carrier medium v/s OSYS, (c) concentration of carrier medium and SiC Particles v/s OSYS, (d) concentration of Fe particles and SiC Particles v/s OSV, (e) concentration of Fe particles and carrier medium v/s OSV, and (f) concentration of carrier medium and SiC Particles v/s OSV.

finishing process where low viscosity in the off-state situation and high yield strength in the on-state situation are required. From TOPSIS analysis, fluid sample 9 is selected as the best alternative from the available samples.

So, it is further employed in the finishing process to investigate its performance. The results of the finishing process carried out for 45 minutes showed a remarkably improved surface finish of the hole with a reduction of 76.55% and 67.36% in the initial R_a and

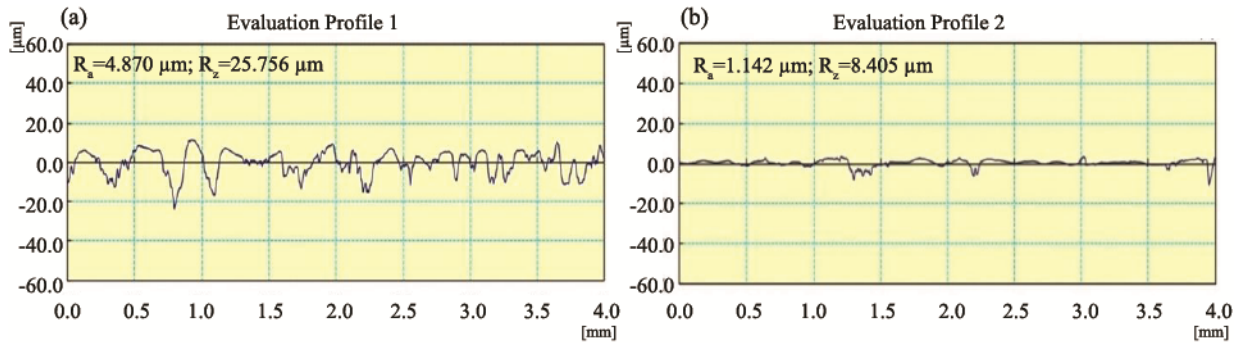


Fig. 12 — (a) Initial surface profile of the hole with R_a and R_z values using fluid sample 9, and (b) Surface profile of the hole after finishing with continuous flow MRFF process with R_a and R_z values using fluid sample 9.

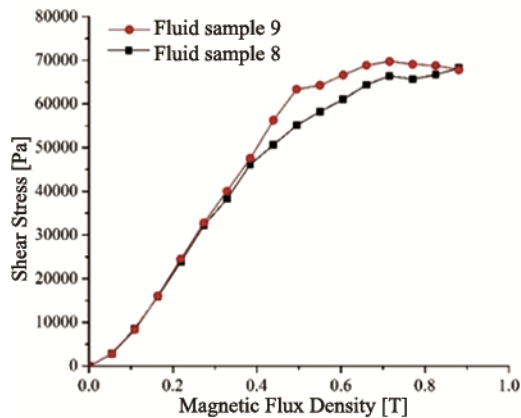


Fig. 11 — Magnetic field v/s yield stress plot for fluid samples 8 and 9.

R_z values respectively. During the process magnetic field is retained at 0.7 T and the flow rate of the fluid is kept at 4 litres/min. Figures 12 (a) exhibits the initial surface profile of the hole with R_a and R_z values of 4.870 μm and 25.756 μm respectively, and Fig. 12 (b) exhibits the surface profile after continuous flow MRFF process with R_a and R_z values of 1.142 μm and 8.405 μm respectively.

4 Conclusion

In present study, MR fluid's rheological characteristics used in the continuous flow MRFF process have been investigated. Sixteen fluid samples having different compositions, designed by Taguchi design of experiment L_{16} OA, are synthesized. All the fluid samples characterized are based upon their OSV and OSYS. In conformity with the experimental studies, the conclusions drawn are as follows:

- The rheological characteristics of prepared MR finishing fluids exhibit that fluid sample #16 has the highest OSYS as 31.23 kPa and fluid sample #2 has the lowest OSV as 0.314 Pa-s.

- From fluid modelling of the fluid samples, Herschel-Bulkley is concluded as the best model with the highest R^2 value of 0.9049 followed by Bingham Plastic and Cason fluid model with R^2 value of 0.7685 and 0.4859 respectively.
- From TOPSIS based multi-response optimization study, fluid sample #9 has been found to have the highest preference value, providing the best multiple response characteristics, hence it has the optimal composition of MR finishing fluid. The optimal parametric combination is summed up to be $A_3B_1C_3D_1$ i.e., “third level of parameter A (Fe powder concentration), first level of B (SiC powder concentration), third level of C (carrier medium concentration) and first level of D (type of carrier medium)”.
- By calculating the mean of the performance values for all the levels of input parameters, the weight percentage of Fe powder has ranked first in deciding the selected multiple responses followed by weight percentage of SiC abrasives, weight percentage of carrier medium and type of carrier medium respectively.
- From ANOVA of preference values, it is also concluded that the Fe powder concentration is the most predominant input parameter which affects the preference value with a contribution of 66.12%, after that SiC abrasives concentration with a contribution of 08.09%, whereas type of carrier medium is the least significant with a contribution of 03.31%.
- From the magnetic field strength v/s OSYS curves, fluid samples #8 and #9, the saturation magnetization of the samples is noticed around a magnetic field intensity of 0.6 to 0.8 Tesla. The fluid samples also attain the highest OSYS in this range of magnetic field, so it should be

considered as the limiting value of magnetic field during the finishing operation.

- Fluid sample #9, having the highest preference value from TOPSIS analysis, has also been employed in the developed continuous flow MRFF process to validate its performance and a significant reduction of 76.55% and 67.36% in the initial R_a and R_z values respectively of surface roughness of the hole has been observed.

Acknowledgements

Authors express gratitude to IIT, Ropar; UIET, Panjab University, Chandigarh and Anton Paar India Pvt. Ltd. Bengaluru, for providing the laboratory facilities to support this research work.

References

- Genç S & Phulé P P, *Smart Mater Struct*, 11 (2002) 316.
- Jolly M R, Carlson J D & Munoz B C, *Smart mater struct*, 5 (1999) 607.
- Phule P P, *Smart Materials Bulletin*, 2 (2001) 7.
- Chaudhuri A, Wereley N M, Kotha S, Radhakrishnan R & Sudarshan T S, *J MagnMagn Mater*, 293 (2005) 206.
- Kumar M, Das M & Yu N, *Nanomanufacturing Metrol*, 5 (2022) 259.
- Mangal S & Kataria M, *J Appl Fluid Mech*, 11 (2018) 1751.
- Paswan S K, Aggarwal A & Singh A K, *Proc Inst Mech Eng, Part E*, 236 (2022) 824.
- Saraswathamma K, Jha S & Rao P V, *Mater Manuf Process*, 30 (2015) 661.
- Yadav R D, Singh A K & Arora K, *J Manuf Process*, 57 (2020) 254.
- Amir M, Mishra V, Sharma R, Iqbal F, Ali S W, Kumar S & Khan G S, *Ceram Int*, 49 (2023) 6254.
- Bedi T S & Singh A K, *Mater and Manuf Process*, 33 (2018) 1141.
- Das M, Jain V K & Ghoshdastidar P S, *Mach Sci Technol*, 14 (2010) 365.
- Gupta M K, Dinakar D, Chhabra I M, Jha S & Madireddy B S, *Optik*, 226 (2021) 165908.
- Kataria M & Mangal S K, *J Braz Soc Mech Sci Eng*, 41 (2019) 551.
- Paswan S K & Singh A K, *Proc Inst Mech Eng Part C*, 234 (2019) 363.
- Dorosti A H, Ghatee M & Norouzi M, *J MagnMagn Mater*, 498 (2020) 166193.
- Ghosh G, Sidpara A & Bandyopadhyay P P, *Precis Eng*, 79 (2023) 221.
- Li S, Tian T, Wang H, Li Y, Li J, Zhou Y & Wu J, *Mater Des*, 194 (2020) 108935.
- Paswan S K & Singh A K, *Wear*, 426 (2019) 68.
- Sirwal S A & Singh A K, *Proc Inst Mech Eng Part C*, 233 (2019) 1541.
- Grover V & Singh A K, *Mater and Manuf Process*, 33 (2018) 1177.
- Jha S & Jain V K, *wear*, 261 (2006) 856.
- Sidpara A, Das M & Jain V K, *Mater and Manuf Process*, 24 (2009) 1467.
- Mangal S K & Sharma V, *J Braz Soc Mech Sci Eng*, 39 (2017) 4191.
- Rosenfeld N, Wereley N M, Radakrishnan R & Sudarshan T S, *Int J Mod Phys B*, 16 (2002) 2392.
- Srivastava M, Pandey P M, Basheed G A & Pant R P, *J MagnMagn Mater*, 534 (2021) 168044.
- Paswan S K, Bedi T S & Singh A K, *Wear*, 376B (2017) 1207.
- Sadiq A & Shunmugam M S, *Int J Mach Tools Manuf*, 49 (2009) 554.
- Roszkowska E, *Multiple Criteria Decision Making*, 6 (2011) 200.
- Chhabra R P & Richardson J F, *Non-Newtonian flow in the process industries: fundamentals and engineering applications* (Elsevier, Netherlands), 1stEdn, ISBN: 978-0-7506-3770-1, 1999, p. 37.
- Macosko C W, *Rheology principles, measurements and applications* (Wiley, USA), 1stEdn, ISBN: 1-56081-579-5, 1994, p.65.
- Dash R K, Mehta K N & Jayaraman G, *Int J Eng Sci*, 34 (1996) 1145.
- Antil P, *Silicon*, 12 (2019) 275.
- Malik A & Manna A, *J Braz Soc Mech Sci Eng*, 40 (2018) 148-1.